Prevalence of Rate-Dependent Behaviors in Cardiac Muscle

G. Martin Hall, Sonya Bahar, and Daniel J. Gauthier

Department of Physics, Department of Biomedical Engineering, and Center for Nonlinear and Complex Systems,
Duke University, Box 90305, Durham, North Carolina 27708

We explore the rate-dependent dynamic response of periodically paced bullfrog (*Rana catesbeiana*) cardiac muscle. Alternans (2:2 behavior) occur in 35% of animals and 2:1 ↔ 1:1 bistability in 74% of animals. In addition, we observe 2:2 ↔ 2:1 bistablility. We discuss the implications of these results for two map-based models of cardiac dynamics. The high prevalence of bistability suggests that this dynamical behavior must be accounted for in the design of closed-loop feedback protocols to stabilize cardiac dynamics. [S0031-9007(99)08837-7]

Spatiotemporal complexity can degrade the performance of dynamical systems. Recent research has focused on the control of complexity in biological systems, where a loss of performance can be deadly [1]. In cardiac function, for example, it is advantageous to suppress the spatiotemporal disorganization of ventricular fibrillation that prevents blood from being pumped throughout the body. Chaos control techniques [2] have shown the potential to modify temporal disorganization in spatially extended cardiac tissue using small electrical perturbations. To optimize the design of these control techniques it is essential to determine the types and prevalence of spatially localized dynamical behaviors that have been correlated with the initiation of spatiotemporal complexity in the heart [3,4].

In this Letter we investigate *in vitro* the response of small pieces of bullfrog (*Rana catesbeiana*) cardiac muscle to periodic electrical stimulation to determine the prevalence of different rate-dependent behaviors. Under various conditions of periodic electrical stimulation (pacing), M stimuli can elicit N responses ($M:N$ behavior). A wide range of these responses have been observed depending on the type of cardiac tissue, animal species, or stimulus parameters, such as frequency [5], amplitude [6], and shape [7]. We concentrate on *rate-dependent* behaviors in cardiac muscle because of the wide range of excitation rates that occur in both healthy and pathological cardiac tissue. In addition, we explore the range of dynamical behaviors in a large number of animals to determine the relative prevalence of different dynamical states because control protocols must be able to deal with every behavior occurring in a population.

We find that bistability between 1:1 and 2:1 patterns exists in 17 of 23, or 74%, of the cardiac preparations. The window of bistability is situated over a range of pacing intervals (or basic cycle length, BCL) that lies near the natural period of the resting heart (∼1000 ms), and extends for ∼160 ms. We find that 2:2 behavior (alternans) occurs in 8 of 23, or 35%, of cardiac preparations. In all cases where 2:2 behavior is observed, bistability also occurs between 2:2 and 2:1 dynamics. We find that the stimulus that does

not elicit a response in the 2:1 state does, in fact, have an effect on the tissue dynamics. Furthermore, we find that the bifurcation to 2:1 behavior is subcritical, and that unstable periodic orbits do not occur for pacing intervals shorter than that at which the tissue undergoes a transition to a 2:1 pattern. Most significantly, our findings indicate that bistability is highly prevalent in bullfrog cardiac tissue, and thus optimal controllers must be designed with sufficient flexibility to deal with bistability as well as unstable periodic orbits.

In these experiments, the heart is excised from adult animals of either sex from 4 to 8 inches in length [8]. After pacemaker cells are cut away, a small piece (≤3 × 3 × 5 mm) of ventricular myocardium is removed, placed in a chamber, and superfused with a recirculated physiological solution. The tissue, quiescent in absence of an applied stimulus, is paced with 4-ms-long square-shaped current pulses applied through two fine (51 μm) tungsten wires set ∼2 mm apart on the surface of the tissue [9]. The amplitude of the applied stimulus is typically ∼0.1− 0.2 mA, twice the current necessary to elicit a response so that we conduct our experiments in a parameter regime where only 1:1, 2:2, and 2:1 dynamics should occur [10,11]. Intracellular (transmembrane) voltages are typically measured within 1−2 mm of the stimulus electrodes using a glass micropipette. Before initiating data collection, the tissue is paced at a BCL of ∼1000 ms for about 20 min.

A typical method for investigating the dynamics of small pieces of cardiac tissue is to measure the time for cells to repolarize after depolarization by a brief electrical stimulus (this time interval is known as the action potential duration, APD) as the interval between stimuli (BCL) is slowly varied. When the tissue is paced slowly, each stimulus elicits one action potential, with all APD equal (1:1 pattern). As the BCL is decreased the tissue reaches a point at which it cannot recover fast enough to respond to every stimulus, entering a 2:1 pattern in which one response occurs for every two stimuli. Occasionally, a 2:2 pattern (responses of alternating duration) intervenes between the 1:1 and 2:1

states [12]. We observe hysteresis between these dynamical states as the pacing interval is swept up and down.

The coexistence of two stable states at the same BCL is seen in Figs. 1a and 1b, where we show the temporal evolution of the transmembrane potential for a BCL of 600 ms. Figure 1a is recorded after the BCL is slowly varied from 1200 to 600 ms, and Fig. 1b is recorded after the BCL is slowly varied from 300 to 600 ms.

A bifurcation diagram is a convenient way to summarize observations of the long-term dynamical behavior of the tissue as BCL is varied slowly. We obtain such a diagram by recording the APD while adjusting the BCL across a wide range of physiological values, from 1200 to 300 ms in 100 or 50 ms intervals (downsweep), and then from 300 to 1200 ms, again in 100 or 50 ms steps (upsweep). For each BCL, the response of the tissue to the first 5–10 stimuli is discarded in order to eliminate transients and the subsequent behavior is recorded for up to 10 sec. After discarding transients, the width of each action potential is determined at 70% of full repolarization and plotted at each BCL.

Figure 2a shows a bifurcation diagram for the experimental preparation in Fig. 1. For long BCLs, the tissue responds in a 1:1 pattern. The APD decreases for decreasing BCL (open circles). As the BCL is decreased from 500 to 400 ms, an abrupt increase in the APD occurs, highlighted by the thin vertical arrow, indicating the bifurcation from a 1:1 to a 2:1 pattern. After the smallest BCL of our pacing protocol is achieved, the BCL is increased slowly (closed

triangles). The tissue remains on the 2:1 branch for a wide range of BCL values that elicited 1:1 response during the downsweep. At a BCL between 700 and 800 ms, the tissue response makes an abrupt transition back to 1:1 behavior. The presence of hysteresis indicates that this transition is a subcritical bifurcation [13].

For some animals, the tissue undergoes a different set of bifurcations, as shown in Fig. 2b. During the downsweep (open circles), a 1:1 → 2:2 transition occurs followed by a bifurcation from 2:2 to the 2:1 branch, indicated by a thin vertical arrow. During the upsweep (closed triangles), the tissue remains on the 2:1 branch, eventually returning to the 1:1 regime. Note that the 1:1 → 2:2 transition is a supercritical Hopf bifurcation, while the 2:2 → 2:1 transition is a subcritical bifurcation, such as the 1:1 → 2:1 transition shown in Fig. 2a. In all tissue preparations that show 2:2 behavior, bistability is also observed. Bistability between 1:1 and 2:1 dynamical states has been reported previously both in periodically paced bullfrog myocardium [14] and spontaneously beating aggregates of embryonic chick heart cells [10]. However, to our knowledge, there has been no prior experimental observation of 2:2 ↔ 2:1 rate-dependent bistability in cardiac tissue, a phenomenon predicted in [5].

The size of the hysteretic windows of various preparations, including regions of 2:2 ↔ 2:1 hysteresis, ranges from 50 to 400 ms, with an average of 157 ± 67 ms. Note, however, that our BCL step size is 50 or 100 ms;
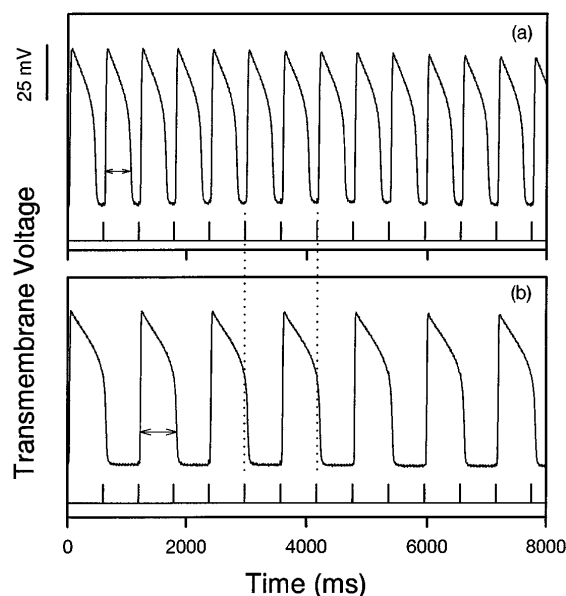

FIG. 1. Temporal evolution of transmembrane potential where the stimulus waveform is shown at the bottom of each diagram. The tissue exhibits (a) 1:1 dynamics for slow pacing during a BCL downsweep and (b) 2:1 dynamics for the same BCL used in (a), but during an upsweep. Arrows indicate measured APD. Vertical dotted lines illustrate the correspondence between stimulus intervals.
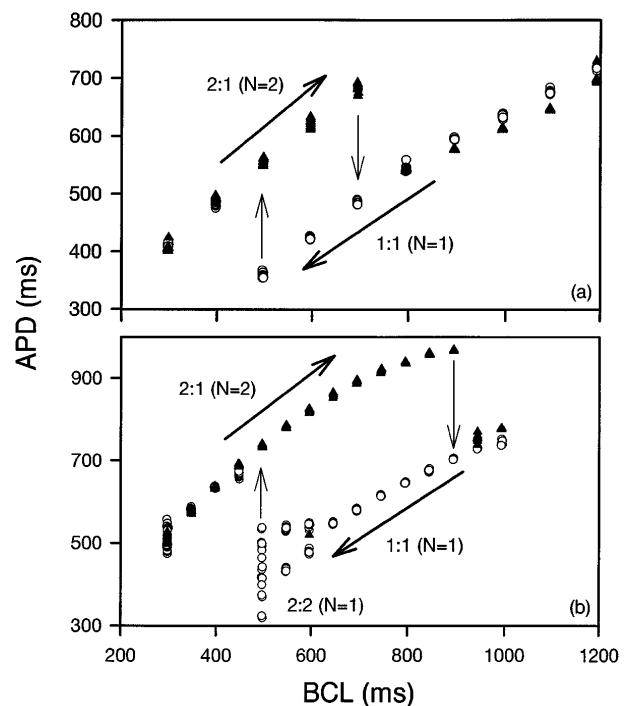

FIG. 2. (a) Bifurcation diagram showing 2:1 ↔ 1:1 hysteresis. Open circles (closed triangles) are APD measurements as the BCL is decremented (incremented). (b) Alternans, bistability, and hysteresis observed for a different animal.

it is possible that animals in which we do not observe hysteresis actually possess hysteretic windows below the resolution of our experiment. In two of the 23 animals, we studied two different pieces of tissue and found that the overall dynamics for both pieces from a single animal were qualitatively similar, though the specific location of the bifurcations varied.

The animal-to-animal variation we observe indicates that both the existence of alternans and the size of the hysteretic window depend sensitively on the tissue characteristics. However, since our experiments are conducted over a number of months, and with animals of various sizes, we conclude that the observed prevalence of bistability is generic in *Rana catesbeiana*. Preliminary experiments indicate that rate-dependent bistability also occurs in a spatially localized region of a periodically paced *in vivo* sheep atrium [15].

Patterns of alternans in the T wave of the electrocardiogram [4], have been correlated with vulnerability to ventricular fibrillation in human patients. Such observations have formed the basis for general models of spatiotemporal instabilities in excitable media [16] as well as more specific models of spatially extended dynamics in cardiac systems [3]. However, the presence of a wide window of bistability between 1:1 (2:2) and 2:1 patterns in cardiac tissue suggests that rate-dependent bistability and hysteresis in cardiac muscle must be considered in the development of techniques for the control or modification of complex cardiac dynamics using small electrical stimuli. Different control schemes may have to be developed to modify dynamics in the neighborhood of different bifurcations.

A qualitative understanding of our observations may be obtained from simple mapping models of localized cardiac dynamics such as that suggested by Nolasco and Dahlen [17] and later generalized by Guevara *et al.* [5]. In such models, the action potential duration APD_{n+1} is typically expressed as

$$\text{APD}_{n+1} = f(N \times \text{BCL} - \text{APD}_n), \qquad (1)$$

where N is the smallest integer satisfying the condition $N \times \text{BCL} - \text{APD}_n > \theta$, and θ is the minimum diastolic interval (DI) the tissue can sustain. Note that the 1:1 and 2:2 patterns observed in the experiments correspond to $N = 1$, and the 2:1 pattern corresponds to $N = 2$. For some tissue preparations, including bullfrog myocardium [17], a function of the form

$$f(\text{DI}_n) = \text{APD}_{\max} - A e^{-\text{DI}_n/\tau} \qquad (2)$$

gives good agreement with experimental observations, where $\text{APD}_{\max}$, A, and τ are tissue-dependent constants and $\text{DI}_n \equiv N \times \text{BCL} - \text{APD}_n$.

To find model parameters which fit the observations shown in Fig. 2a, we require that the model undergoes 1:1 → 2:1 and 2:1 → 1:1 transitions at the observed BCL values, and that the model does not undergo a bifurcation

to a 2:2 state. Figure 3 shows a comparison between our experimental observations shown in Fig. 2a and the theoretically predicted bifurcation diagram generated using the simple mapping (solid lines) given by Eqs. (1) and (2). While the bifurcations occur at the correct BCL values, there is a significant discrepancy in the observed and predicted values of the APDs. Note that no unstable periodic orbits exist for DI $< \theta$ in this model.

It is also important to note that this simple model is exquisitely sensitive to small parameter changes. Decreasing τ by as little as 10% yields a map that bifurcates to 2:2 behavior before the transition to the 2:1 branch. This underscores the potential pitfall of adhering to rigid choices of parameter regimes when developing or implementing models of biological systems.

We have investigated the discrepancy between the simple one-dimensional model and the observed data, and find that it is impossible to find a smooth function f that depends only on DI_n that both fits accurately the data of the $N = 1$ branch and reproduces the appropriate bifurcation diagram. This can be seen in Fig. 4, which shows the dependence of f on DI_n for the data displayed in Fig. 2a. It is seen that one value of DI can give rise to two different values of APD, depending on whether the tissue response is on the $N = 1$ (solid line) or $N = 2$ (dotted line) branch. Thus the stimulus that does not elicit a response in the 2:1 pattern does in fact alter the tissue dynamics, and the observed data cannot be described by a single-valued function. Furthermore, the observed stability of the 1:1 branch is inconsistent with the fit to the $N = 1$ (solid line) branch using Eqs. (1) and (2). The 1:1 pattern generated by the model must be unstable when the slope of f is greater than unity. However, the observed 1:1 pattern is stable when the rate of decrease in APD with respect to a decrease in DI is larger than unity.

To correctly account for the observed stability, a model must include at least one other dynamical variable. The
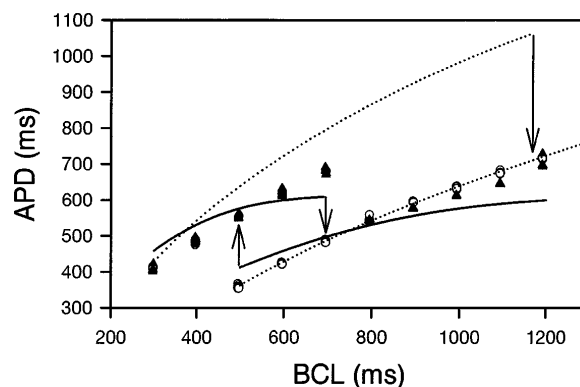

FIG. 3. Fits to the bifurcation diagram shown in Fig. 2a. The solid line is obtained by iterating (1) and (2) using $\text{APD}_{\max} = 616$ ms, $A = 313$ ms, $\tau = 207$ ms, and $\theta = 86$ ms. The dotted line is obtained using (3) with $c_1 = 1359$ ms, $c_2 = 2.64$, $\tau_1 = 51$ ms, $\tau_2 = 1080$ ms, and $\theta = 136$ ms.
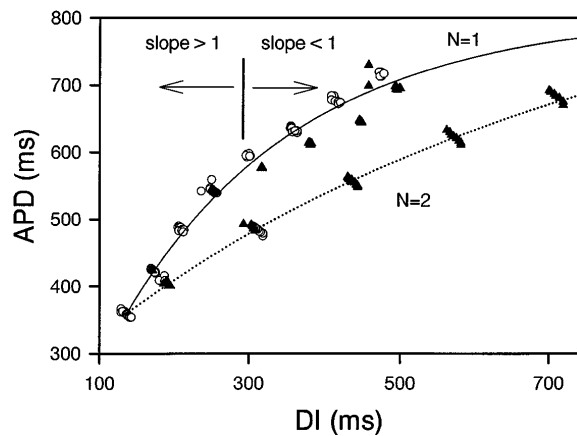
FIG. 4. Action potential duration as a function of diastolic interval for data shown in Fig. 2a. Open circles indicate downsweep; closed triangles indicate upsweep. The data separates into two distinct branches corresponding to $N = 1$ and $N = 2$. The vertical line at DI = 285 ms indicates the diastolic interval at which the slope of the $N = 1$ branch becomes greater than unity. Solid (dotted) curve illustrates the $N = 1$ ($N = 2$) branch.

difference-differential model, proposed by Chialvo and Jalife [11], includes a memory term M describing the long-term evolution of the tissue properties. With certain simplifications, this model reduces to

$$\mathrm{APD}_{n+1} = c_1(1 - M_n)\big[1 - c_2 e^{-(N \times \mathrm{BCL} - \mathrm{APD}_n)/\tau_1}\big],$$
$$M_{n+1} = \big[1 + (M_n - 1)e^{-\mathrm{APD}_n/\tau_2}\big]e^{-(N \times \mathrm{BCL} - \mathrm{APD}_n)/\tau_2}, \tag{3}$$

with N determined as above. A least squares fit of the fixed points of (3) to our data on the $N = 1$ branch (open circles in Fig. 2a) is illustrated by the dotted lines in Fig. 3. This model clearly fits the $N = 1$ branch data better than the simpler model and hence correctly predicts stable 1:1 behavior even though the slope of the APD versus DI curve is greater than 1. However, there is little agreement between the model and observed APD values on the $N = 2$ branch, and the transition from the $N = 2$ to the $N = 1$ branch occurs at a much longer BCL than that found experimentally. This suggests that significant improvements must be made to this model before it can completely describe the experimentally observed results.

We gratefully acknowledge the Whitaker Foundation for financial support.

[1] L. Glass, Phys. Today **49**, 40 (1996).

[2] A. Garfinkel, M. L. Spano, W. L. Ditto, and J. L Weiss, Science **257**, 1230 (1992); D. J. Christini and J. J. Collins, Phys. Rev. E **53**, R49 (1996); K. Hall, D. J. Christini, M. Tremblay, J. J. Collins, L. Glass, and J. Billette, Phys. Rev. Lett. **78**, 4518 (1997).

[3] A. Karma, Chaos **4**, 461 (1994).

[4] R. L. Verrier and B. D. Nearing, in *Cardiac Electro-physiology: from Cell to Bedside,* edited by D. P. Zipes and J. Jalife (Saunders, Philadelphia, 1995), Chap. 45, 2nd ed.; B. Surawicz and C. Fisch, J. Am. Coll. Cardiol. **20**, 483 (1992); M. A. Murda'h, W. J. McKenna, and A. J. Camm, PACE **20**, 2641 (1997).

[5] M. Guevara, G. Ward, A. Shrier, and L. Glass, *Computers in Cardiology* (IEEE Computer Society, Silver Springs, MD, 1984), pp. 167–170.

[6] M. Landau, P. Lorente, J. Henry, and S. Canu, J. Math. Biol. **25**, 491 (1987); P. Lorente and J. Davidenko, Ann. NY Acad. Sci. **591**, 109 (1990).

[7] J. Hescheler and R. Speicher, Eur. Biophys. J. **17**, 273 (1989).

[8] Bullfrogs are anesthetized using 1% wt/vol 3-aminobenzoic acid ethyl ester mixed with cold tap water, double pithed, and dissected by cutting along the ventral side of the body. Physiological solution (100 ml/min flow rate) is maintained at temperature $20 \pm 2\,°\mathrm{C}$ and contains 110 mM NaCl, 2.7 mM KCl, 1.5 mM $MgCl_2$, 1.8 mM $CaCl_2$, 5.6 mM glucose, 2.8 mM Na_2HPO_4, and 1 mM HEPES. It is buffered with $NaHCO_3$ and bubbled continuously with 95% O_2 and 5% CO_2 to maintain a pH of 7.4 ± 0.1. To reduce motion of the tissue due to contractions, 5–20 mM 2-3-butanedione monoxime (DAM) is added. DAM does not affect the gross dynamical features of this preparation.

[9] All procedures are approved by the Duke University Institutional Animal Care and Use Committee (IACUC).

[10] M. Guevara, A. Shrier, and L. Glass, in *Cardiac Electro-physiology: from Cell to Bedside,* edited by D. P. Zipes and J. Jalife (Saunders, Philadelphia, 1990), Chap. 23, 1st ed.

[11] D. R. Chialvo, D. C. Michaels, and J. Jalife, Circ. Res. **66**, 525 (1990); D. R. Chialvo and J. Jalife, in *Cardiac Electrophysiology: from Cell to Bedside,* edited by D. P. Zipes and J. Jalife (Saunders, Philadelphia, 1990), Chap. 24, 1st ed.

[12] D. R. Chialvo and J. Jalife, Nature (London) **330**, 749 (1987); M. Watanabe, N. F. Otani, and R. F. Gilmour, Circ. Res. **76**, 915 (1995).

[13] P. Berge, Y. Pomeau, and C. Vidal, *Order Within Chaos: Towards a Deterministic Approach to Turbulence* (Wiley, New York, 1984), pp. 40–42.

[14] G. R. Mines, J. Phys. (London) **46**, 349 (1913).

[15] R. Oliver, G. M. Hall, S. Bahar, W. Krassowska, P. Wolf, E. Dixon-Tulloch, and D. J. Gauthier (unpublished).

[16] A. Karma, Nature (London) **379**, 118 (1996).

[17] J. B. Nolasco and R. W. Dahlen, J. Appl. Phys. **25**, 191 (1968).